

Contact Mechanics of a Small Icosahedral Virus

Cheng Zeng, Mercedes Hernando-Pérez, and Bogdan Dragnea*
Department of Chemistry, Indiana University, Bloomington, Indiana 47405, USA

Xiang Ma
Department of Chemistry, Idaho State University, Pocatello, Idaho 83209, USA

Paul van der Schoot†
Department of Applied Physics, Eindhoven University of Technology, P.O. Box 513, 5600 MB Eindhoven, Netherlands

Roya Zandi
*Department of Physics and Astronomy, University of California at Riverside,
900 University Avenue, Riverside, California 92521, USA*
(Received 26 January 2017; published 20 July 2017)

A virus binding to a surface causes stress of the virus cage near the contact area. Here, we investigate the potential role of substrate-induced structural perturbation in the mechanical response of virus particles to adsorption. This is particularly relevant to the broad category of viruses stabilized by weak noncovalent interactions. We utilize atomic force microscopy to measure height distributions of the brome mosaic virus upon adsorption from solution on atomically flat substrates and present a continuum model that captures our observations and provides estimates of elastic properties and of the interfacial energy of the virus, without recourse to indentation.

DOI: [10.1103/PhysRevLett.119.038102](https://doi.org/10.1103/PhysRevLett.119.038102)

The problem of how adhesion of a deformable object to a surface is driven by interfacial energy and opposed by elasticity is at the center of modern contact mechanics [1], and instances of it can be found in variety of settings, including biophysical phenomena. For example, cell membranes are naturally impermeable to virus particles. For viruses to cross plasma, endosomal, or nuclear membranes, the virus-cell interface has to change drastically after virus adsorption [2]. This is often done in a system-specific manner [3,4]. Nevertheless, before specific transformations take place, virus particles must stick at the apical cell surface via generic interactions, e.g., hydrophobic or electrostatic [5]. Could this initial random binding event already perturb the mechanochemistry of the virus particle in a way that would prime it for the next sequence in the entry process? Gao *et al.* have suggested a model for the clathrin-independent endocytosis mechanism by which interactions between ligands fixed on the particle surface and free receptors on the plasma membrane would result in bringing more of the membrane into contact with the particle, which, in turn, would lead to the particle being eventually engulfed by the plasma membrane [6]. This receptor-mediated wrapping mechanism model was revisited to allow particles to deform under the influence of adhesion to the flexible membrane surface, which materialized in a potentially strong effect of particle contact mechanics on the cellular uptake [7]. Furthermore, more recent experimental studies provided indication that, at least in certain cases, virus stiffness may regulate entry [8].

In contact mechanics of small soft-material particles, solid surface tension is believed to dominate elasticity [9]. At the same time, while virus deformation upon adsorption on substrates for atomic force microscopy (AFM) has been occasionally observed [10–14], it has not been studied in detail, and contributions of solid surface tension have not been investigated. Here, we report on a case study aiming to determine quantitatively how virus mechanics responds to virus adsorption to a surface. We find that a small icosahedral plant virus, the brome mosaic virus (BMV), will bind to atomically flat surfaces predominantly in one orientation, and that, in order to achieve this preferred orientation, it will deform mainly at the contact interface. Indentation experiments suggest that the spring constant of the virus remains largely unaffected by the local substrate-induced deformation. In other words, local stresses due to surface binding and distortion do not seem to propagate to the top, where the measurement is done. Furthermore, with the aid of an elastic model including surface tension contributions, we show how the distribution of particle heights on the substrate can inform on the magnitudes of elastic moduli and of the contact surface energy, without recourse to indentation experiments.

Viruses are obligated biological systems much smaller than cells but still composed of hundreds to tens of thousands of molecules working together. A complete understanding of their dynamic properties requires a unifying framework including contributions from scale-dependent and scale-independent phenomena [15]. In

recent years, studies of virus mechanics under the influence of an external perturbation have begun to shed light on how energy flows between the different degrees of freedom of these complex molecular assemblies. For instance, osmotic pressure assays have provided new clues on how chemical energy is transformed into mechanical energy for phage genome injection [16], and single molecule pulling experiments with optical tweezers have helped elucidating the mechanisms of phage genome packaging [17–19].

In the category of *in singulo* methods based on mechanical force application, AFM indentation [20] has allowed the measurement of virus and protein cage deformation under a uniaxial load [21,22] and of the relationship between virus mechanics and chemistry, which includes contributions from environmental factors [23] and from the nucleic acid cargo [20,24–26].

In AFM, for sufficient imaging resolution and to perform reproducible indentation experiments, particles have to be immobilized strongly enough to resist lateral forces exerted by the probe [27]. Noncontact AFM imaging is generally considered as being the least intrusive [28–30]. Even then, while mean forces during imaging are usually below 0.1 nN, peak force estimates in “tapping” mode can exceed 0.1 nN (albeit for only ~ 1 ms per pixel) [31]. Such forces require either virus immobilization in a crystalline lattice [32] or strong adhesion forces between the virus and substrate when probing single viruses. It is for this reason that, in practice, substrates are usually prepared by coating with ligands apt at binding virus particles [33,34].

Upon adsorption, an equilibrium is established between external adhesion forces and the cohesive interactions within the virus. While adhesion-induced deformation was observed before [10–13], very little is actually known about this equilibrium. How does the balance between adhesion and mechanical stresses affect particle shape? How large is the adhesion area at equilibrium? What is the magnitude of surface energy? Does surface adhesion result in local structural perturbations that propagate through the virus lattice up to the top, at the indentation area? This study takes on addressing such questions on one of the most-studied virus systems adsorbed on chemically well-defined atomically flat substrates.

BMV was the first virus imaged by AFM at capsomeric resolution [35]. It is an established model [36] for small (+) single-stranded RNA icosahedral viruses, the most plentiful viruses on this planet [37]. BMV has a nonenveloped capsid formed from 180 copies of the same coat protein (CP), organized in a $T = 3$ lattice with an average outer diameter of 284 Å [38]. The outer surface of the BMV capsid is studded with hydrophobic patches surrounded by polar residues (Supplemental Material, Fig. 1 [39]) and thus, BMV readily adsorbs on both hydrophobic surfaces and polar surfaces.

In this Letter, we study maximum particle height distributions measured by AC-mode AFM onto atomically flat

surfaces of two materials: highly oriented pyrolytic graphite (HOPG) and mica. The idea is that adhesion forces will tend to maximize the contact area by locally flattening the virus at the contact point. Assuming that, for small perturbations, the part of the virus particle in contact with the liquid behaves approximately as an elastic shell [21], an increase in the contact area can be accomplished at the energetic cost of bending the shell and of forming a rim, which we define as the locus where the fluid, the substrate, and the outer surface of the shell meet. As a result, the maximum height of the virus over the surface support changes upon adsorption. Since measuring height is done relative to the substrate, it was beneficial to utilize atomically flat and chemically homogeneous substrates for this work, as opposed to the rougher functionalized etched glass substrates sometimes used in indentation experiments, in particular, for BMV and its close relative, cowpea chlorotic mottle virus (CCMV) [34,45,46]. Chemically homogeneous substrates such as HOPG and mica minimize inhomogeneous broadening of the adhesive interaction strength.

Height measurements can be affected not only by substrate roughness, but also by virus shell anisotropy. For BMV, the root-mean-square deviation (rmsd) from a spherical surface is ~ 20 Å [47]. Since the measurement is made top down, it is important to record virus particle orientation relative to the substrate. Imaging at the experimental conditions reported here (see Supplemental Material [39]) leads to sufficient lateral resolution (Supplemental Material, Fig. 2) to distinguish not only broad icosahedral symmetry features, but also individual capsomers on the virus surface [Fig. 1(a)]. In these conditions, we find orientational bias on both substrates.

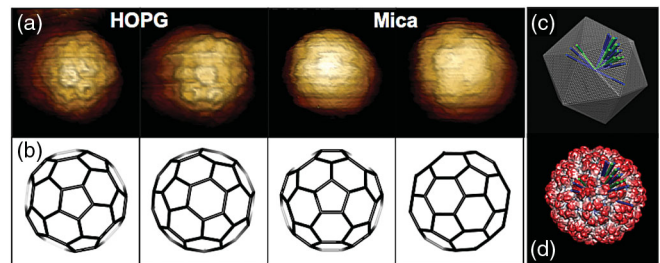


FIG. 1. (a) AFM images of BMV particles adsorbed on HOPG and mica at sufficient resolution to distinguish broad morphological features from a single capsomer ~ 6 nm in size. Scale bars: 10 nm. (b) Orientations of model icosahedra that correspond to virus particle orientations in (a). (c),(d) Distribution of surface normal directions, estimated from single measurements and represented as colored lines mapped onto the icosahedron and onto the BMV molecular model (HOPG: green, $N = 17$ particles; mica: blue, $N = 21$ particles). Note: minimum spacing between bars does not represent the actual resolution in estimating capsid orientation; the angular uncertainty is approximately 5° (see Supplemental Material [39] for methods, which includes Refs. [34,40–44].)

Among particles of sufficient resolution for orientation determination, the most frequent orientation is with a threefold axis normal to the substrate ($\sim 70\%$ of a total of 38 particles with sufficient resolution to be unambiguously analyzed), as shown in Figs. 1(d) and 1(e). Note that, in subsequent experimental runs (using one tip), we either resolve capsomer arrangement on most of the particles or on none of them, which suggests that obtaining spatial resolution is mainly determined by probe sharpness and not by particle characteristics. Moreover, if particles were adsorbed with random orientation, one would expect the threefold axis orientation to be observed less often. Early work on the cowpea chlorotic mottle virus done on KOH etched glass and silanized glass found random capsid orientations, in contrast with our findings [20]. The difference may come from the fact that etched glass is more rough and chemically heterogeneous. As a consequence, particles may bind upon landing with an enhanced initial contact area and hence, with stronger initial adhesion and little subsequent reorientation. The situation is likely different on atomically flat chemically homogenous surfaces, where an initial small contact would, in general, require reorientation to avoid desorption. Orientational selection could come from the most exposed areas on the virus surface having a pronounced hydrophobic character and affinity for non-polar surfaces such as HOPG (Supplemental Material, Fig. 1). Moreover, anionic residue patches bordering these areas may bind to divalent cations [such as Mg(II) present in buffer solution] and adsorbed on the mica surface [48].

When a single orientation dominates, one would expect a narrow distribution of maximum heights on the substrate, corresponding to that orientation. However, measurement of BMV maximum heights on HOPG and mica shows that on both substrates, height histograms peak at values 3–4 nm below the nominal 28.4 nm for BMV [Supplemental Material, Fig. 3(a)]. Moreover, histograms are asymmetric, with the longer tail extending towards lower heights, while the greater heights wing ends abruptly in the vicinity of the nominal BMV diameter. Height distribution, peak position and peak width depend on the substrate, suggesting a chemical effect. Note that a small (5 Å) correction to the apparent height values was made to account for compression under the imaging force (see Supplemental Material [39]) [34].

Lower heights than the nominal diameter suggest particle deformation upon adhesion, [Supplemental Material, Fig. 3(b)]. Since BMV particles have elastic constants of ~ 0.2 N/m, the compression force that would have to act on the virus to obtain a deformation associated with the observed drop in height of ~ 3 –4 nm is ~ 500 (mica) to 600 pN (HOPG). Flattening is overall stronger on HOPG than mica. Notably, resolution is also higher on HOPG, Fig. 1, which may be due to the stronger grip by HOPG and thus, smaller positional fluctuations under imaging. This value gives an order of magnitude estimate of

substrate-induced interactions at work. Interestingly, buckling forces are not very far (800–1000 pN) from this value, but this is not very surprising as recent work showed that the stiff particles of the adeno-associated virus can be partially crushed by adsorption on a hydrophobic substrate [14].

An analytical model was set up that captures in a formal, albeit heuristic way, the interplay between elastic properties, capsid deformation, and adhesion. The model is inspired by the Helfrich treatment of the elastic properties of lipid bilayers [49] but with significant differences as a viral shell is a different object than a lipid vesicle. A specific assumption is made that, upon landing on a surface, adhesion can increase by local deformation and formation of a flat contact area (base) with circular symmetry (Supplemental Material, Fig. 4). In other words, there is a sharp boundary or fracture between the flat surface base and the spherical cap, in solution. We opted for this geometry instead of the one assuming continuous deformation of membrane vesicles adsorbed on a surface [50] because, due to the discrete nature of shell subunits, line fracture rather than continuous deformation is a reasonable assumption. Moreover, a continuously deformed particle should become prestressed by adsorption and presumably, as a consequence, show changes in apparent stiffness, a situation which, as we will see later, we do not observe. Finally, a continuously deformed particle having a smooth surface has zero contributions to the elastic energy from the Gaussian curvature, which, as we shall see, would lead to unrealistic values for material constants.

Area stretching or compression would imply deformation of the proteins and/or increase in capsomeric surface-to-surface distances. Both processes are expensive, the latter on account of the short-ranged nature of the interactions [51]. Attempts to fit the data including an area stretching or compression term indicated that contributions from net area stretching or compression could be neglected. Area conservation upon deformation is thus assumed, which leads to a relationship between height and the cap radius: $a = \sqrt{(4r_0^2 - h^2)}/2$, where r_0 is the initial particle radius, and h is the height on the surface after binding and deformation (Supplemental Material, Fig. 4). The spherical cap radius then obeys (Supplemental Material, Fig. 4): $r = (4r_0^2 + h^2)/4h$.

The total energy is partitioned into contributions from the bending and Gauss energies, as well as a surface energy associated with the contact area and a line or rim energy associated with the contact perimeter. The total energy is (see Supplemental Material [39]):

$$F = \frac{1}{2}\kappa\left(\frac{2}{r} - \frac{2}{r_0}\right)^2 2\pi rh + 2\pi\kappa_G \frac{h}{r} - \gamma\pi a^2 + \tau 2\pi a, \quad (1)$$

where κ is the bending modulus, κ_G is the Gauss modulus, γ is the surface energy, and τ is the rim energy.

Within the thin shell approximation, the Gauss and bending moduli are related via Poisson's ratio [52]: $\kappa_G = \kappa(\nu - 1)$. For small icosahedral ssRNA viruses, $\nu \approx 0.3-0.4$ [20,26,53]. Here, we take the value $\nu = 0.3$. The free energy change upon adsorption can be then written as a sole function of the reduced height $H = h/2r_0$. Parameters κ , κ_G , γ , and τ can be then, in principle, found from fitting experimental data with a Boltzmann distribution derived from the free energy as a function of H [Eq. (1)].

We attempted to fit the data without the Gaussian term and in the presence of stretching energy. When we remove the Gauss term, we obtain a substrate-dependent bending modulus, which should have been a property determined by the nature of the virus rather than the underlying surface. Furthermore, unreasonably high values for the bending modulus were observed in this instance (see Supplemental Material [39]). The expression given in Eq. (1) is the simplest equation with which we are able to fit the experimental data.

It is important to note that the Gauss term would have a vanishing contribution on a continuous surface topologically equivalent to a sphere [50]. Since no Gauss term yielded unrealistic results, we made the assumption that, unlike for vesicles, in our case, the surface is not differentiable everywhere, and hence, the Gauss term does contribute to the total free energy change. If we keep the Gauss term, then our data could be fitted using the same values for the bending modulus on different substrates. The fitting results and parameters for these conditions are summarized in Fig. 2 and Table 1, Supplemental Material. As discussed in the following, parameter values agree well with those previously reported by other methods.

Since the bending of a shell involves compression of the inner surface and extension of the outer surface, the bending modulus κ is related to the stretching modulus κ_s through $\kappa = \kappa_s w^2/\alpha$, where w is the shell thickness, and

$\alpha = 12, 24$, or 48 , depending on the shell model (12 for a uniform plate [52], 24 for a polymer brush [54], 48 for a two-leaflet structure [55]). For virus capsids, $\alpha = 12$ has been previously used [56–58], which, in our case, leads to $\kappa_s \approx 43 k_B T/nm^2$. In an examination of the low-frequency modes of a very similar virus to BMV, the chlorotic cowpea mosaic virus (CCMV), May *et al.* calculated, in the context of a spherical harmonic basis set, κ_s values for the $l = 0$ and $l = 1$ modes at $81 k_B T/nm^2$ and $60 k_B T/nm^2$, respectively [59]. Note that while in AFM indentation experiments, the $l = 1$ is the dominating mode, both $l = 0$ and $l = 1$ modes are likely to be required in order to describe deformation in our case. Thus, estimates for the bending modulus from the particle height data lead to comparable values with those previously reported from similar systems.

From the relation between the particle height, initial radius, and radius of the flat part of the adsorbed virus, we can find the base area that corresponds to the most probable particle height. The base radius for HOPG is ≈ 9 nm, and the corresponding base area is ≈ 250 nm². Creating the base lowers the particle energy by $\approx 40 k_B T$ with a rim contribution of $\approx 5 k_B T$. Note that different contributions dominate at different height ranges. For instance, the rim contribution dominates when the contact area is small. Populations at $h \approx 2r_0$ are determined by the magnitude (and sign) of τ . More specifically, a barrier to adsorption would occur if τ is positive (see Supplemental Material, Fig. 5). Such seems to be the case on HOPG but not on mica (see Supplemental Material, Table 1).

As area conservation is assumed, it is not necessary to include a stretching term in our model. However, to verify how reliable this assumption is, we relaxed the constant area constraint (see Supplemental Material [39] for details). This necessitates the introduction of a stretching term in the free energy expression in order to account for the energy cost associated with any changes in the surface area. For simplicity, uniform stretching was assumed for the entire shell, and the stretching modulus κ_s was related to the bending modulus as we have seen above. Fitting of the height histogram with the relaxed area constraint leads to a total surface area decrease for both HOPG and mica substrates. Still, the bending modulus showed negligible change. These results suggest that the contribution from stretching is minimal and that the assumption of constant surface area is reasonable.

Together, our findings on the orientation bias and the estimates for the contact area suggest a possible mechanism for adsorption. We have seen that the most probable orientation on HOPG and mica is with a threefold axis normal to the substrate. Considering the magnitude of the radius for the contact area, pentamers should be located on its circumference, i.e., touching the substrate. Keeping in mind that previous indentation experiments suggest compression to occur more readily along a threefold than along a fivefold axis [58] and that hexameric interfaces are

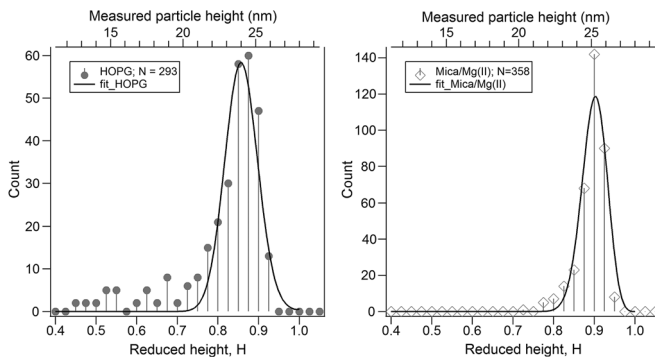


FIG. 2. Model fit of the particle height distribution on HOPG (a) and mica (b), plotted with respect to particle height (top axis) and reduced height (bottom axis). At close to nominal heights ($H = 1$), contact area is minimal and the likelihood of desorption increased; thus, populations are low. At smaller heights, adhesion comes at the cost of structural perturbation, modeled here as elastic.

thought to fail more readily than pentameric ones [60,61], we propose that the main displacement upon adsorption occurs along the threefold axis, with the hexamer at the center radially shifting its position from the surface towards the particle center and with the stiffer pentamers acting as a stabilizing tripod. As the interfacial area grows, a point is reached where the cost of continuing the flattening of the shell is greater than the energy drop due to adhesion, at which point, the virus shell is stabilized.

It is worth noting that normal mode analysis of the mechanical properties of icosahedral virus capsids [62] predicts pentamers to have greater propensity to move freely. However, continuum approaches based on elastic theory predict in certain cases the opposite, i.e., pentamers being stiffer than hexamers [63]. The latter is valid for large ratios between elastic and bending energy contributions, for large viruses, and when spontaneous curvature effects can be neglected [64]. It would be interesting to see how the inclusion of substrate effects might affect these analyses. In any case, our experiments seem to support a scenario with stiffer pentamers, at least for BMV.

An issue of practical importance from a measurement perspective is whether interactions at the substrate-virus interface affect readings of the virus stiffness in AFM indentation experiments. We have performed AFM indentation on BMV adsorbed on HOPG in a buffer solution (see Supplemental Material [39] for experimental details) and plotted the elastic constants as a function of particle height. Within the framework of the proposed model, the smaller the height, the larger the virus-substrate interaction. Do particle height and elastic constants correlate? As expected, the joint histogram presented in Fig. 5, Supplemental Material suggests that, within the experimental uncertainty, this is not the case. The particle height varied independently of the measured elastic constant K_v , which remained constant at 0.20 ± 0.06 N/m. Interestingly, this would also be expected within the framework of thin shell theory [51]. Note that, for the simple thin shell model, the elastic constant K_v is proportional to the Young's modulus, which, in turn, is directly proportional to the bending modulus κ . To avoid inhomogeneous broadening of K_v in this experiment and keep experimental uncertainty low, we produced a nearly homogeneous BMV virion population containing mainly a subset of the viral genome ($\sim 90\%$ of RNA3/4) via an engineered *Agrobacterium* expression system [65]. Moreover, natural variation in the average radius of the virus particle (from cryoelectron microscopy measurements) is ~ 1 nm, much smaller than the deviations measured here.

In conclusion, we have utilized AFM imaging in solution on flat chemically homogeneous substrates to show that the orientation and height of viruses adsorbed on a substrate depend on the virus-substrate interaction. BMV appears to adsorb preferentially with a threefold axis parallel to the surface normal. Local deformation, measurable as a change

in virus height, ensues as elastic and adhesive forces equilibrate. A simple model fitting experimental data suggests that interfacial energies of tens of $k_B T$ accompany the encounter of BMV with both charged and nonpolar model substrates. As we used the simplest possible free energy to obtain insights into the contribution of different elastic energies, our model is highly approximate, and it cannot reproduce the long tail in the distribution. The long tail includes particles that have been most flattened upon interaction with the substrate, i.e., particles for which contact mechanics is presumably nonlinear and scale dependent. Further investigations are required. However, local deformation at the contact area does not change the apparent elastic constant as measured by AFM indentation, which suggests that curvature elastic stress does not change upon adsorption. Since it appears that virus orientation and deformation at the surface stabilize interfacial interactions, an interesting question that might be raised is that of anisotropic deformability as yet another biologically beneficial facet of icosahedral symmetry in viruses.

This work has been supported by the U.S. Department of Energy, Office of Science, Basic Energy Sciences, under Award No. DE-SC0010507 (to B. D.), by the U.S. Army Research Office under Award No. W911NF-13-1-0490 (to B. D.), by the Human Frontier Science Program, under Award No. RGP0017/2012 (to B. D. and P. v. d. S.), and the National Science Foundation (No. DMR-1310687 to R. Z.). The authors thank Dr. Irina Tsvetkova for her critical reading of the manuscript.

*dragnea@indiana.edu

†Present and permanent address: Institute for Theoretical Physics, Utrecht University, Princetonplein 5, 3584 CC Utrecht, Netherlands.

- [1] D. Maugis, *Contact, Adhesion, and Rupture of Elastic Solids* (Springer, Berlin, 1999).
- [2] U. F. Greber, *J. Virol.* **90**, 3802 (2016).
- [3] L. Li, J. Jose, Y. Xiang, R. J. Kuhn, and M. G. Rossmann, *Nature (London)* **468**, 705 (2010).
- [4] T. S. Jardetzky and R. A. Lamb, *Curr. Opin. Virol.* **5**, 24 (2014).
- [5] J. Mercer, M. Schelhaas, and A. Helenius, *Annu. Rev. Biochem.* **79**, 803 (2010).
- [6] H. J. Gao, W. D. Shi, and L. B. Freund, *Proc. Natl. Acad. Sci. U.S.A.* **102**, 9469 (2005).
- [7] X. Yi, X. Shi, and H. Gao, *Phys. Rev. Lett.* **107**, 098101 (2011).
- [8] H.-B. Pang, L. Hevroni, N. Kol, D. M. Eckert, M. Tsvitov, M. S. Kay, and I. Rousso, *Retrovirology* **10**, 4 (2013).
- [9] R. W. Style, C. Hyland, R. Boltyanskiy, J. S. Wettlaufer, and E. R. Dufresne, *Nat. Commun.* **4**, 2728 (2013).
- [10] M. Knez, M. P. Sumser, A. M. Bittner, C. Wege, H. Jeske, D. M. P. Hoffmann, K. Kuhnke, and K. Kern, *Langmuir* **20**, 441 (2004).
- [11] A. Llauró, E. Coppari, F. Imperatori, A. R. Bizzarri, J. R. Castón, L. Santi, S. Cannistraro, and P. J. de Pablo, *Biophys. J.* **109**, 390 (2015).

- [12] A. Llauro, D. Luque, E. Edwards, B. L. Trus, J. Avera, D. Reguera, T. Douglas, P. J. de Pablo, and J. R. Castón, *Nanoscale* **8**, 9328 (2016).
- [13] A. Llauro, B. Schwarz, R. Koliyatt, P. J. de Pablo, and T. Douglas, *ACS Nano* **10**, 8465 (2016).
- [14] C. Zeng, S. Moller-Tank, A. Asokan, and B. Dragnea, *J. Phys. Chem. B* **121**, 1843 (2017).
- [15] R. Phillips and S. R. Quake, *Phys. Today* **59**, No. 5, 38 (2006).
- [16] W. M. Gelbart and C. M. Knobler, *Phys. Today* **61**, No. 1, 42 (2008).
- [17] D. E. Smith, S. J. Tans, S. B. Smith, S. Grimes, D. L. Anderson, and C. Bustamante, *Nature (London)* **413**, 748 (2001).
- [18] P. K. Purohit, J. Kondev, and R. Phillips, *Proc. Natl. Acad. Sci. U.S.A.* **100**, 3173 (2003).
- [19] D. E. Smith, *Curr. Opin. Virol.* **1**, 134 (2011).
- [20] J. P. Michel, I. L. Ivanovska, M. M. Gibbons, W. S. Klug, C. M. Knobler, G. J. L. Wuite, and C. F. Schmidt, *Proc. Natl. Acad. Sci. U.S.A.* **103**, 6184 (2006).
- [21] W. H. Roos, R. Bruinsma, and G. J. L. Wuite, *Nat. Phys.* **6**, 733 (2010).
- [22] C. Carrasco, A. Luque, M. Hernando-Pérez, R. Miranda, J. Carrascosa, P. Serena, M. de Ridder, A. Raman, J. Gómez-Herrero, I. Schaap, D. Reguera, and P. de Pablo, *Biophys. J.* **100**, 1100 (2011).
- [23] B. D. Wilts, I. A. Schaap, and C. F. Schmidt, *Biophys. J.* **108**, 2541 (2015).
- [24] C. Carrasco, A. Carreira, I. A. T. Schaap, P. A. Serena, J. Gómez-Herrero, M. G. Mateu, and P. J. de Pablo, *Proc. Natl. Acad. Sci. U.S.A.* **103**, 13706 (2006).
- [25] R. Vaughan, B. Tragesser, P. Ni, X. Ma, B. Dragnea, and C. C. Kao, *J. Virol.* **88**, 6483 (2014).
- [26] A. Ahadi, D. Johansson, and A. Evilevitch, *J. Biol. Phys.* **39**, 183 (2013).
- [27] M. Baclayon, G. J. L. Wuite, and W. H. Roos, *Soft Matter* **6**, 5273 (2010).
- [28] P. K. Hansma, J. P. Cleveland, M. Radmacher, D. A. Walters, P. E. Hillner, M. Bezanilla, M. Fritz, D. Vie, H. G. Hansma, C. B. Prater, J. Massie, L. Fukunaga, J. Gurley, and V. Elings, *Appl. Phys. Lett.* **64**, 1738 (1994).
- [29] F. Moreno-Herrero, P. de Pablo, M. Álvarez, J. Colchero, J. Gómez-Herrero, and A. Baró, *Appl. Surf. Sci.* **210**, 22 (2003).
- [30] D. Martinez-Martin, C. Carrasco, M. Hernando-Perez, P. J. de Pablo, J. Gomez-Herrero, R. Perez, M. G. Mateu, J. L. Carrascosa, D. Kiracofe, J. Melcher, and A. Raman, *PLoS One* **7**, e30204 (2012).
- [31] X. Xu, C. Carrasco, P. J. de Pablo, J. Gomez-Herrero, and A. Raman, *Biophys. J.* **95**, 2520 (2008).
- [32] Y. Kuznetsov, A. Malkin, T. Land, J. DeYoreo, A. Barba, J. Konnerth, and A. McPherson, *Biophys. J.* **72**, 2357 (1997).
- [33] D. J. Müller, M. Amrein, and A. Engel, *J. Struct. Biol.* **119**, 172 (1997).
- [34] W. H. Roos, *Methods Mol. Biol.* **783**, 251 (2011).
- [35] Y. G. Kuznetsov, A. J. Malkin, R. W. Lucas, M. Plomp, and A. McPherson, *J. Gen. Virol.* **82**, 2025 (2001).
- [36] C. C. Kao and K. Sivakumaran, *Mol. Plant Pathol.* **1**, 91 (2000).
- [37] S. J. Flint, L. Enquist, V. Racaniello, and A. Skalka, *Principles of Virology: Molecular Biology*, 3rd ed. (ASM Press, Washington, DC, 2009).
- [38] Z. Wang, C. F. Hryc, B. Bammes, P. V. Afonine, J. Jakana, D.-H. Chen, X. Liu, M. L. Baker, C. Kao, S. J. Ludtke, M. F. Schmid, P. D. Adams, and W. Chiu, *Nat. Commun.* **5**, 4808 (2014).
- [39] See Supplemental Material at <http://link.aps.org/supplemental/10.1103/PhysRevLett.119.038102> for details of experimental method, manuscript supporting figures, and analytical model.
- [40] R. Lipowsky and U. Seifert, *Langmuir* **7**, 1867 (1991).
- [41] E. F. Pettersen, T. D. Goddard, C. C. Huang, G. S. Couch, D. M. Greenblatt, E. C. Meng, and T. E. Ferrin, *J. Comput. Chem.* **25**, 1605 (2004).
- [42] W. Roos, R. Bruinsma, and G. Wuite, *Nat. Phys.* **6**, 733 (2010).
- [43] J. N Israelachvili, *Intermolecular and Surface Forces*, 3rd ed (Academic Press, Burlington, MA, 2011), p. 450.
- [44] P. Ni, Z. Wang, X. Ma, N. C. Das, P. Sokol, W. Chiu, B. Dragnea, M. Hagan, and C. C. Kao, *J. Mol. Biol.* **419**, 284 (2012).
- [45] J. Michel, I. Ivanovska, M. Gibbons, W. Klug, C. Knobler, G. Wuite, and C. Schmidt, *Proc. Natl. Acad. Sci. U.S.A.* **103**, 6184 (2006).
- [46] B. D. Wilts, I. A. Schaap, and C. F. Schmidt, *Biophys. J.* **108**, 2541 (2015).
- [47] R. W. Lucas, S. B. Larson, and A. McPherson, *J. Mol. Biol.* **317**, 95 (2002).
- [48] H. Hansma and D. Laney, *Biophys. J.* **70**, 1933 (1996).
- [49] W. Helfrich, *Z. Naturforsch. C* **28**, 693 (1973).
- [50] U. Seifert and R. Lipowsky, *Phys. Rev. A* **42**, 4768 (1990).
- [51] M. Buenemann and P. Lenz, *Proc. Natl. Acad. Sci. U.S.A.* **104**, 9925 (2007).
- [52] L. Landau and E. M. Lifshitz, *Theory of Elasticity*, 3rd ed. (Elsevier Science, Amsterdam, 1984).
- [53] M. M. Gibbons and W. S. Klug, *Biophys. J.* **95**, 3640 (2008).
- [54] W. Rawicz, K. Olbrich, T. McIntosh, D. Needham, and E. Evans, *Biophys. J.* **79**, 328 (2000).
- [55] D. Boal, *Mechanics of the Cell* (Cambridge University Press, Cambridge, England, 2002).
- [56] M. M. Gibbons and W. S. Klug, *Phys. Rev. E* **75**, 031901 (2007).
- [57] J. Cuellar, F. Meinhoevel, M. Hoehne, and E. Donath, *J. Gen. Virol.* **91**, 2449 (2010).
- [58] W. H. Roos, M. M. Gibbons, A. Arkhipov, C. Uetrecht, N. R. Watts, P. T. Wingfield, A. C. Steven, A. J. R. Heck, K. Schulten, W. S. Klug, and G. J. L. Wuite, *Biophys. J.* **99**, 1175 (2010).
- [59] E. R. May, A. Aggarwal, W. S. Klug, and C. L. Brooks, *Biophys. J.* **100**, L59 (2011).
- [60] R. Zandi and D. Reguera, *Phys. Rev. E* **72**, 021917 (2005).
- [61] V. Krishnamani, C. Globisch, C. Peter, and M. Deserno, *Eur. Phys. J. Spec. Top.* **225**, 1757 (2016).
- [62] F. Tama and C. L. Brooks, *J. Mol. Biol.* **345**, 299 (2005).
- [63] M. Buenemann and P. Lenz, *Phys. Rev. E* **78**, 051924 (2008).
- [64] J. Lidmar, L. Mirny, and D. R. Nelson, *Phys. Rev. E* **68**, 051910 (2003).
- [65] P. Ni, R. C. Vaughan, B. Tragesser, H. Hoover, and C. C. Kao, *J. Mol. Biol.* **426**, 1061 (2014).